IJRCS

International Journal of Robotics and Control Systems
Vol. 4, No. 2, 2024, pp. 480-501
ISSN 2775-2658
http://pubs2.ascee.org/index.php/ijrcs

ASCEE

Adaptive Controller Based on Estimated Parameters for Quadcopter Trajectory Tracking

Sophyn Srey [a,1,*], Sarot Srang [a,2]

[a] Dynamic and Control Laboratory, MIT Research Unit, Institute of Technology of Cambodia, Cambodia
[1] sophynkh@gmail.com; [2] srangsarot@itc.edu.kh
[*] Corresponding Author

ARTICLE INFO

Article History
Received 7 March 2024
Revised 11 April 2024
Accepted 29 April 2024

Keywords
Quadcopter;
Simplified Rotational Dynamics;
Lumped Parameter;
UKF;
Estimation;
Adaptive Controller;
Trajectory Tracking

ABSTRACT

This paper presents a trajectory control system design for a quadcopter, an unmanned aerial vehicle (UAV), which is based on estimated parameters that are assumed to exhibit random walk behavior. Initially, the rotational dynamic model of the UAV is formulated using the Newton Euler method in terms of angular velocity about the x, y, and z axes. This model is then simplified into three separated-first-order linear differential equations, with coefficients derived from the combined effects of inertia, aerodynamic drag, and gyroscopic effects, referred to as lumped parameters. A Proportional-Integral (PI) controller with feed-forward design is then developed to control this simplified model. To adapt the controller to the lumped parameters that exhibit random walk behavior, each simplified equation is restructured into a processing and measurement model. The states of these models are estimated by using the Unscented Kalman Filter (UKF). These estimated values are then utilized to adjust the PI gains and compensate the signal of the designed angular velocity controller, transforming it into an adaptive controller. The entire UAV controller comprises two main parts, an inner loop for adaptive angular rate control and an outer loop serving as an attitude-thrust controller. The proposed controller is simulated using Simulink, with circular and square trajectories. The simulation results demonstrate that the quadcopter successfully follows the desired circular and square paths. The steady-state error for the x and y axes in the square trajectory is less than 0.05 meters within 5 seconds, and for the z axis, it is less than 0.02 meters within 2.5 seconds. The controller gains do not require adjustment when changing trajectories. Moreover, the estimated parameters remain nearly constant at steady state.

1. Introduction

Quadcopters have been used as favorite vehicles to perform tasks which are dangerous or impossible for humans to complete, such as photography, agriculture, surveillance, communications, search and rescue operations, and military applications [1]-[4]. Within these operations, handling heavy payloads and stabilizing horizontal and altitude tracking positions in predefined areas are the most significant applications. To achieve these tasks, several control algorithms have been reported in the literature [5]-[8]. The most common techniques are to control the quadcopter by linearizing the dynamic model around a hovering point and applying PID control techniques to allow UAV to follow the desired paths as reported in [9]-[13]. This controller performs well for a step-desired path but struggles when the trajectory deviates from the linearized point such as curving path. Nonlinear control

algorithms such as feedback linearization, backstepping, sliding mode, model predictive controller as studies in [13]-[22] employ complex computational approaches like the Lyapunov function to ensure the errors of desired states asymptotically approach zero. Despite studies reporting the effectiveness of these controllers for quadcopters to follow complex paths in simulations and physical experiments, it is challenging to tune values that make the errors of the states approach zero while adhering to the Lyapunov concept. Moreover, it is not adaptive when desired paths change. It is observed that all the mentioned controllers, the structure of UAVs is symmetric, allowing the decoupling of moment inertia to be canceled out, which simplifies the dynamic model calculation. No studies report the control of rotational dynamic motion by any controllers. However, in practice, tracking performance of quadcopter always suffers from uncertain parameters such as non-symmetry of structure design or small structure deformation during operation which cause the decoupling of inertia occurring in rotational dynamic motion, variation of payload with time caused by wind, changing paths or other external disturbance.

The core controller in study is the adaptive controller for rotational dynamic model of UAV where its structure is assumed to be non-symmetric or small deformation occurring during operation. The rotational dynamic model of UAV is derived for angular velocity. Then it is simplified as first-order linear differential equations, where their coefficients are lumped relevant parameters such wind disturbance, inertia or gyroscopic effect and they behave random walking. A PI controller is proposed to control the simplified equation. To estimated those lumped parameters which are changing, the derived models are remodeled into nonlinear differential equation of processing model and measuring model. The states of the remodels are to be estimated by the unscented Kalman filter (UKF) during operation to use for tuning PI gains and to compensate the signal for angular velocity controller to be adaptive. These PI gains and compensated values are changing according to the estimated values. This responds to the mentioned uncertainties and it is also enable UAV to track different paths without changing the controller gains. In this adaptive controller, the real model is preferred rather than the simplified model.

The first contribution of this work is the derived rotational dynamic model and the first-order simplified differential equation with the coefficients as lumped parameters. The second contribution is the remodels of the simplified models for estimating the lumped parameters and the adaptive controller that controls the angular velocity of the UAV to perform in three axes simultaneously. The third contribution is the whole control system of the UAV that allows it to carry heavy payloads and track many paths without changing the controller gains. .

The next parts of this paper are organized as follows. In Section 2, coordinate frame, transformation matrix and derived rotational dynamic model of the UAV are established with lumped parameters. In Section 3, the control system for the rotational dynamic model is presented, following by implementation of UKF algorithm. The derived equation is remodeled to estimate the lumped states and parameters for designing an adaptive control system for UAV to maneuver in three axis simultaneously. In section 4, the entire process for designing controller is described. In Section 5, the performances of the designed control system are assessed and the estimated parameters are discussed. Conclusion is given in Section 6.

2. Flight Dynamics of Quadcopter

Quadcopter is a type of UAV that is able to fight vertically, forward, backward, rightward, leftward and hover by using the speed of four propellers to produce thrust and torques about x, y and z axes. In this study, the four propellers are placed on $(x-y)$ plane in cross-configuration as depicted in Fig. 1. To eliminate coupling, the first and third propellers are paired and set to rotate in the same anticlockwise direction, while the second and fourth propellers are paired and set to rotate in the same clockwise direction. To manipulate the four typical maneuvers of quadcopter motion, the speed of

each propeller is controlled as followings. For vertical motion, the speed of the four propellers is increased or decreased to produce thrust that is greater or less than gravity. Backward and forward motion are manipulated by increasing the speed of the second and third propellers faster or slower than the speed of the first and fourth propellers. Rightward and leftward motion are manipulated by increasing the speed of the first and second propellers faster or slower than the speed of the third and fourth propellers [23] and [24]. In this study, the quadcopter is assumed to be non-symmetric structure and may be deformation during operation, which cause the inertia decoupling and cannot cancel out for rotational dynamic motion. Also, the center mass gravity of the quadcopter is assumed to coincide with the center of geometry.

2.1. Coordinate Frames and Kinematic Equation of Motion

Motion of a quadcopter involves three main right-hand referent coordinate frames as shown in Fig. 1. The North-East-Down (NED) orthogonal coordinate frame is set at a fixed earth frame whose origin is the take-off point. This frame is also called an inertial coordinate frame $\mathcal{F}_E = (o_E, x_E, y_E, z_E)$ and used as reference for trajectory tracking.The $\mathcal{F}_b = (o_b, x_b, y_b, z_b)$ is a moving orthogonal body frame whose origin is attached to the center mass of the UAV. In this frame, positive $o_b x_b$ axis points out the front face, positive $o_b y_b$ axis points out the right side of UAV and positive $o_b z_b$ axis points down the center gravity of earth. Another intermediate frame is the vehicle coordinate frame $\mathcal{F}_v$, whose origin coincides with the body frame but whose axes are aligned with the axes of the inertial frame or NED frame [25] and [26]. Table 1 lists names of state variables and parameters used in the study.

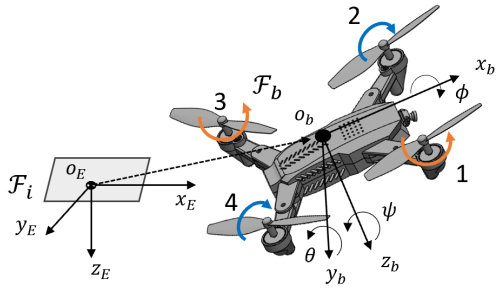

Fig. 1. Coordinate frames of quadcopter

Table 1. States and parameters

Symbols	Definitions	Units
$\mathbf{X} = (x, y, z)^\top$	linear position vector in $\mathcal{F}_i$	m
$\mathbf{X}_d = (x_d, y_d, z_d)^\top$	linear desired position vector in $\mathcal{F}_i$	m
$\boldsymbol{\eta} = (\phi, \theta, \psi)^\top$	Angular position vector in $\mathcal{F}_v$	rad
$\mathbf{V} = (u, v, w)^\top$	linear velocity vector in $\mathcal{F}_b$	m/s
$\boldsymbol{\omega} = (p, q, r)^\top$	Angular velocity vector in $\mathcal{F}_b$	rad/s
$\mathbf{M} = (M_x, M_y, M_z)^\top$	Moment vector in $\mathcal{F}_b$	$N.s$
$\mathbf{D} = (D_x, D_y, D_z)^\top$	Drag coefficient vector in $\mathcal{F}_b$	$N.s/s^2$
g	gravitational acceleration	m/s^2
m	Total mass of UAV	Kg

Transformation matrix from the vehicle frame $\mathcal{F}_v$ to the body frame $\mathcal{F}_b$ is given by three successive rotation matrices $\mathcal{R}_v^b(\phi, \theta, \psi)$, where $\boldsymbol{\eta} = (\phi, \theta, \psi)^\top$ are commonly called Euler angles. The first rotation is about z-axis by yaw angles ψ, the second rotation is about the moved y-axis by pitch angle θ, and the final rotation is about moved x-axis by roll angle ϕ [27] and [28]. These rotation matrices are defined as following,

$$\mathcal{R}_v^b(\psi) = \begin{bmatrix} \cos\psi & \sin\psi & 0 \\ -\sin\psi & \cos\psi & 0 \\ 0 & 0 & 1 \end{bmatrix}, \mathcal{R}_v^b(\theta) = \begin{bmatrix} \cos\theta & 0 & -\sin\theta \\ 0 & 1 & 0 \\ \sin\theta & 0 & \cos\theta \end{bmatrix}, \mathcal{R}_v^b(\phi) = \begin{bmatrix} 1 & 0 & 0 \\ 0 & \cos\phi & \sin\phi \\ 0 & -\sin\phi & \cos\phi \end{bmatrix}.$$

The transformation matrix $\mathcal{R}_v^b(\phi,\theta,\psi)$ from vehicle frame to body frame is defined as:

$$\begin{aligned} \mathcal{R}_v^b(\phi,\theta,\psi) &= \mathcal{R}_v^b(\phi)\mathcal{R}_v^b(\theta)\mathcal{R}_v^b(\psi) \\ &= \begin{bmatrix} c_\theta c_\psi & -c_\theta s_\psi & s_\theta \\ c_\phi s_\psi + s_\phi s_\theta c_\psi & c_\theta c_\psi - s_\phi s_\theta s_\psi & s_\phi c_\theta \\ s_\phi s_\psi - c_\phi s_\theta c_\psi & s_\phi c_\psi + c_\phi s_\theta s_\psi & c_\phi c_\theta \end{bmatrix} \end{aligned} \tag{1}$$

and transformation matrix $\mathcal{R}_b^v(\psi,\theta,\phi)$ from body frame to vehicle frame is defined as:

$$\begin{aligned} \mathcal{R}_b^v(\psi,\theta,\phi) &= \mathcal{R}_v^b(\psi)\mathcal{R}_v^b(\theta)\mathcal{R}_v^b(\phi) \\ &= \begin{bmatrix} c_\theta c_\psi & s_\phi s_\theta c_\psi - c_\phi s_\psi & s_\phi s_\psi + c_\phi s_\theta c_\psi \\ c_\theta s_\psi & c_\phi c_\psi + s_\phi s_\theta s_\psi & c_\phi s_\theta s_\psi - s_\theta c_\psi \\ -s_\theta & s_\phi c_\theta & c_\phi c_\theta \end{bmatrix} \end{aligned} \tag{2}$$

where $s_x = sin(x)$, and $c_x = cos(x)$.

Relationship between linear velocity vector $\dot{\mathbf{X}} = (\dot{x},\dot{y},\dot{z})^\top$ in initial frame and linear velocity vector $\mathbf{V} = (u,v,w)^\top$ in body frame is carried out by using eq.(2) as following,

$$\begin{aligned} \dot{\mathbf{X}} = \begin{bmatrix} \dot{x} \\ \dot{y} \\ \dot{z} \end{bmatrix} &= R_b^v \mathbf{V} = (R_v^b)^\top \begin{bmatrix} u \\ v \\ w \end{bmatrix} \\ &= \begin{bmatrix} c_\theta c_\psi & s_\phi s_\theta c_\psi - c_\phi s_\psi & c_\phi s_\theta c_\psi + s_\phi s_\psi \\ c_\theta s_\psi & s_\phi s_\theta s_\psi + c_\phi c_\psi & c_\phi s_\theta s_\psi - s_\phi c_\psi \\ -s_\theta & s_\phi c_\theta & c_\phi c_\theta \end{bmatrix} \begin{bmatrix} u \\ v \\ w \end{bmatrix} \end{aligned} \tag{3}$$

Relationship between Euler angle rate $\dot{\boldsymbol{\eta}} = (\dot{\phi},\dot{\theta},\dot{\psi})^\top$ and angular velocity $\boldsymbol{\omega} = (\omega_x,\omega_y,\omega_z)^\top = (p,q,r)^\top$ is carried out as following,

$$\begin{aligned} \begin{bmatrix} p \\ q \\ r \end{bmatrix} &= \begin{bmatrix} \dot{\phi} \\ 0 \\ 0 \end{bmatrix} + \mathcal{R}_v^b(\phi) \begin{bmatrix} 0 \\ \dot{\theta} \\ 0 \end{bmatrix} + \mathcal{R}_v^b(\phi)\mathcal{R}_v^b(\theta) \begin{bmatrix} 0 \\ 0 \\ \dot{\psi} \end{bmatrix} \\ &= \begin{bmatrix} 1 & 0 & -\sin\theta \\ 0 & \cos\phi & \sin\phi\cos\theta \\ 0 & -\sin\phi & \cos\phi\cos\theta \end{bmatrix} \begin{bmatrix} \dot{\phi} \\ \dot{\theta} \\ \dot{\psi} \end{bmatrix}. \end{aligned} \tag{4}$$

Inverting the eq.(4) gives

$$\begin{bmatrix} \dot{\phi} \\ \dot{\theta} \\ \dot{\psi} \end{bmatrix} = \begin{bmatrix} 1 & \sin\theta\tan\theta & \cos\phi\tan\theta \\ 0 & \cos\phi & -\sin\theta \\ 0 & \sin\phi\sec\theta & \cos\phi\sec\theta \end{bmatrix} \begin{bmatrix} p \\ q \\ r \end{bmatrix}. \tag{5}$$

2.2. UAV Equation of Motion

The dynamic equations of the UAV are derived by using Newton's second law of motion in translational and rotational motions in the inertial fixed frame. The equations are given by:

$$\mathbf{F} = \frac{d(m\mathbf{V})}{dt_i}, \tag{6}$$

$$\mathbf{M} = \frac{d(J\boldsymbol{\omega})}{dt_i}, \tag{7}$$

where $\mathbf{F}$ is the sum of all external force vector, m is the constant mass, $\mathbf{V}$ is translational velocity vector, mV is the linear momentum vector, $\mathbf{J}$ is constant inertia vector, $\mathbf{M}$ is the sum of all external moment vectors, $\boldsymbol{\omega}$ is angular velocity vector, $\mathbf{J}\boldsymbol{\omega}$ is the angular momentum vector about the center of gravity of the UAV. Since most measurements are made to be used in body frame, the expression of these equations in the moving body frame is defined as follows,

$$\mathbf{F}_b = m\frac{d\mathbf{V}}{dt_b} + \boldsymbol{\omega} \times m\mathbf{V} = m\dot{\mathbf{V}} + \boldsymbol{\omega} \times m\mathbf{V} \tag{8}$$

$$\mathbf{M}_b = \mathbf{J}\frac{d\boldsymbol{\omega}}{dt_b} + \boldsymbol{\omega} \times \mathbf{J}\boldsymbol{\omega} = \mathbf{J}\dot{\boldsymbol{\omega}} + \boldsymbol{\omega} \times \mathbf{J}\boldsymbol{\omega}, \tag{9}$$

where $\mathbf{V}$ and $\boldsymbol{\omega}$ are defined in body frame.

2.3. Simplified Rotational Dynamic Model

To derive the rotational dynamic model of UAV into first order linear differential equation, the rotational dynamic model in eq.(9) is rearranged into angular velocity form as below:

$$\dot{\boldsymbol{\omega}} = \begin{bmatrix} \dot{\omega}_x \\ \dot{\omega}_y \\ \dot{\omega}_z \end{bmatrix} = \begin{bmatrix} \dot{p} \\ \dot{q} \\ \dot{r} \end{bmatrix} = \mathbf{J}^{-1}\left(-\boldsymbol{\omega} \times \mathbf{J}\boldsymbol{\omega} + \mathbf{M}_b\right) \tag{10}$$

where

$$\boldsymbol{\omega} = \begin{bmatrix} \omega_x \\ \omega_y \\ \omega_z \end{bmatrix} = \begin{bmatrix} p \\ q \\ r \end{bmatrix}, \mathbf{J} = \begin{bmatrix} J_x & -J_{xy} & -J_{xz} \\ -J_{xy} & J_y & -J_{yz} \\ -J_{xz} & -J_{yz} & J_z \end{bmatrix},$$

$$\boldsymbol{\omega} \times = \begin{bmatrix} 0 & -\omega_z & \omega_y \\ \omega_z & 0 & -\omega_x \\ -\omega_y & \omega_x & 0 \end{bmatrix}, \mathbf{M} = \begin{bmatrix} \tau_x \\ \tau_y \\ \tau_z \end{bmatrix} - \begin{bmatrix} \tau_{ax} \\ \tau_{ay} \\ \tau_{az} \end{bmatrix} - \begin{bmatrix} \tau_{gpx} \\ \tau_{gpy} \\ \tau_{gpy} \end{bmatrix},$$

where

$\begin{bmatrix} \tau_{ax} \\ \tau_{ay} \\ \tau_{az} \end{bmatrix}$ is aerodynamic torsional drag and $\begin{bmatrix} \tau_{gpx} \\ \tau_{gpy} \\ \tau_{gpy} \end{bmatrix}$ is gyroscopic torque.

Here, we assume that structure of quadcopter is unsymmetry or when operation the UAV undergoes small deformation which causes the structure of UAV become unsymmetry. This makes the decoupling moments of inertia I_{ab} is not zero. Fully expanding the eq.(10) with their respective components of the above matrix gives

$$\begin{bmatrix}\dot{p}\\ \dot{q}\\ \dot{r}\end{bmatrix} = \begin{bmatrix}\frac{1}{J_x}(J_{xy}r - J_{xz}q)p\\ \frac{1}{J_y}(J_{yz}p - J_{xy}r)q\\ \frac{1}{J_z}(J_{xz}q - J_{xy}p)r\end{bmatrix} + \begin{bmatrix}\frac{1}{J_x}(\tau_x)\\ \frac{1}{J_y}(\tau_y)\\ \frac{1}{J_z}(\tau_z)\end{bmatrix} + \begin{bmatrix}\frac{1}{J_x}(-\tau_{ax} - \tau_{gpx})\\ \frac{1}{J_y}(-\tau_{ay} - \tau_{gpy})\\ \frac{1}{J_z}(-\tau_{az} - \tau_{gpz})\end{bmatrix} + \begin{bmatrix}\frac{1}{J_x}\{(J_y - J_z)rq + J_{yz}(q^2 - r^2) - J_{xy}\dot{q} - J_{xz}\dot{r}\}\\ \frac{1}{J_y}\{(J_y - J_x)rp + J_{xz}(p^2 - r^2) - J_{xy}\dot{p} - J_{yz}\dot{r}\}\\ \frac{1}{J_z}\{(J_y - J_x)pq + J_{xy}(q^2 - p^2) - J_{xz}\dot{p} - J_{yz}\dot{q}\}\end{bmatrix}. \tag{11}$$

The key of estimating random walking parameters by using powerful filters such as UKF is to group relevant unknown parameters and include them as parts of states of model. Then use that filter to estimate their values. Since the body rate p, q, r of UAV are not vary significantly, to simplify the rotational dynamics of UAV, let the following parameters into groups and randomly walk:

$$a = \begin{bmatrix}a_x\\ a_y\\ a_z\end{bmatrix} = \begin{bmatrix}-\frac{1}{J_x}(J_{xy}r - J_{xz}q)\\ -\frac{1}{J_y}(J_{yz}p - J_{xy}r\\ -\frac{1}{J_z}(J_{xz}q - J_{xy}p)\end{bmatrix}, b = \begin{bmatrix}b_x\\ b_y\\ b_z\end{bmatrix} = \begin{bmatrix}\frac{1}{J_x}\\ \frac{1}{J_y}\\ \frac{1}{J_z}\end{bmatrix},$$

$$c = \begin{bmatrix}c_x\\ c_y\\ c_z\end{bmatrix} = \begin{bmatrix}\frac{1}{J_x}(-\tau_{ax} - \tau_{gpx}) - \frac{1}{J_x}\{(J_y - J_z)rq + J_{yz}(q^2 - r^2) - J_{xy}\dot{q} - J_{xz}\dot{r}\}\\ \frac{1}{J_y}(-\tau_{ay} - \tau_{gpy}) - \frac{1}{J_y}\{(J_y - J_x)rp + J_{xz}(p^2 - r^2) - J_{xy}\dot{p} - J_{yz}\dot{r}\}\\ \frac{1}{J_z}(-\tau_{az} - \tau_{gpz}) - \frac{1}{J_z}\{(J_y - J_x)pq + J_{xy}(q^2 - p^2) - J_{xz}\dot{p} - J_{yz}\dot{q}\}\end{bmatrix}, \tau = \begin{bmatrix}\tau_x\\ \tau_y\\ \tau_z\end{bmatrix}.$$

We propose to simplify eq.(9) as first order differential equations in term of angular velocities and external moment as following about x-axis, y-axis and z-axis respectively,

$$\begin{bmatrix}\dot{\omega}_x\\ \dot{\omega}_y\\ \dot{\omega}_z\end{bmatrix} = \begin{bmatrix}-a_x\omega_x + b_x\tau_x - c_x\\ -a_y\omega_y + b_y\tau_y - c_y\\ -a_z\omega_z + b_z\tau_z - c_z\end{bmatrix} \tag{12}$$

where

$$a = \begin{bmatrix}a_x\\ a_y\\ a_z\end{bmatrix}, b = \begin{bmatrix}b_x\\ b_y\\ b_z\end{bmatrix}, c = \begin{bmatrix}c_x\\ c_y\\ c_z\end{bmatrix} \text{ are lumped parameters.}$$

3. Adaptive Controller With Estimated Random Parameters

In the study [29] and [30], the authors derived and simplified the DC motor model into a first order differential equation by lumping parameters. Extended Kalman Filter (EKF) and Unscented Kalman Filter (UKF) were used to estimate those parameters which are constant values to design the PD controllers in one axis rotational dynamic motion by using root locus techniques. In this study, the lumped parameters $a_x, b_x, c_x, a_y, c_y, c_y, a_z, b_c, c_z$ are not constants but they are randomly walking according to $\mathbf{J}, p, q, r, \dot{p}, \dot{q}$ as well as $\dot{r}$. To deal with these behaviors, the study uses parameters estimated from the simplified rotational dynamic model eq.(12) to design rotational dynamic controller for quadcopter flying in three axes simultaneously by deploying UKF to estimate the above random parameters.

3.1. Rotational Dynamic Controller

In the general form of simplified dynamic model shown in eq.(13), the parameters a, b and c are unknown random walking parameters to be estimated, u is input and ω is output,

$$\dot{\omega} = -a\omega + bu - c. \tag{13}$$

This study proposes a PI controlling system as shown in Fig. 2 to control the output ω for rotational dynamic model in eq.(13). It is observed that the term $\frac{c}{b}$ is compensated in the controller signal to cancel the term $(-c)$ in the dynamic model. The expression $\frac{a}{b}\omega_d$ and $\frac{1}{b}\dot{\omega}_d$ are used to adjust the terms ω_d and $\dot{\omega}_d$ into the error and time derivative error for the controlling purpose.The simplified dynamic model eq.(13) in the block diagram can be written as,

$$\dot{\omega} = -a\omega + bk_p e_\omega + bk_i \frac{e_\omega}{s} + a\omega_d + \dot{\omega}_d.$$

Take time derivative on both sides of above equation and let $\dot{e}_\omega = \omega_d - \omega, \ddot{e}_\omega = \dot{\omega}_d - \dot{\omega}$, we obtain the standard form of second order differential as following,

$$\ddot{e}_\omega + (a + bk_p)\dot{e}_\omega + bk_i e_\omega = 0$$
$$\ddot{e}_\omega + 2\xi\omega_n \dot{e}_\omega + \omega_n^2 e_\omega = 0$$

where damping ratio $\xi = a + bk_p$ and natural frequency $\omega_n = \sqrt{bk_i}$. The gains of the PI controllers can be tuned with $k_p = \frac{2\xi\omega_n - a}{b}, k_i = \frac{\omega_n^2}{b}$ by choosing damping ratio such as $\xi = 1$ when the system is critically damped and fastest response together with appropriate natural frequency ω_n as discussed in the studies [31] and [32].

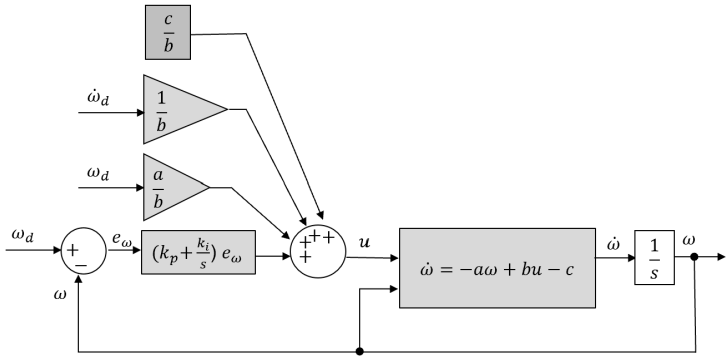

Fig. 2. Rotational dynamic controller

3.2. Unscented Kalman Filter

In this study, we prefer to use the Unscented Kalman Filter(UKF) rather than other filters is that the UKF is able to estimate states of a discrete system that behaves high nonlinearity and respond fast stability. It provides stable estimated parameters in short period that is suitable for online control such UAV dynamic motion. It has been popularly used to estimate the states of UAVs as reported in [33]-[36]. The state space model in discrete system form is defined as:

$$x_k = F(x_{k-1}, u_{k-1}) + \sqrt{Q_d} v_{k-1}$$
$$y_k = H(x_k, u_k) + \sqrt{R} w_k$$

where x_k is state, y_k is the measurement, F is the nonlinear system model, H is the nonlinear measurement model, Q_d is the process noise covariance, v_k is th process noise, R is the measurement noise covariance, and w_k is the measurement noise. As studies in [37]-[39], the UKF algorithm is defined through unscented transformation (UT) to propagate a random variable X (dimensional L) through a nonlinear function $Y = g(X)$, in which X has mean $\bar{X}$ and covariance $\boldsymbol{P}_x$. To obtain statistical values of Y, create a matrix $\mathcal{X}$ of $(2L + 1)$ sigma vectors $\mathcal{X}_i$ corresponding to weights W_i

as follows:

$$\begin{aligned}
\mathcal{X}_0 &= \bar{X} \\
\mathcal{X}_i &= \bar{X} + (\sqrt{(L+\lambda)P_X})_i \;\; i = 1, ..., L \\
\mathcal{X}_i &= \bar{X} - (\sqrt{(L+\lambda)P_X})_i \;\; i = L+1, ..., 2L \\
W_0^{(m)} &= \frac{\lambda}{L+\lambda} \\
W_0^{(c)} &= \frac{\lambda}{L+\lambda+1-\alpha^2+\beta} \\
W_m^i &= \frac{1}{2(L+\lambda)} \;\; i = 1, ..., 2L
\end{aligned}$$

where $\lambda = \alpha^2(L+k)L$ is a scaling parameter. The estimated measurement matrix $\mathcal{Y}_i$ is computed by transforming the $sigma$ vectors $\mathcal{X}$ through the nonlinear measurement model as follows:

$$\mathcal{Y}_i = H(\mathcal{X}_i) \;\; i = 0, ..., 2L.$$

The mean measurement and covariance measurement for Y are approximated by using a weighted sample mean and covariance of the posterior sigma points as follows:

$$\bar{Y} \approx \sum_{i=0}^{2L} W_i^{(m)} \mathcal{Y}_i, \;\; P_Y \approx \sum_{i=0}^{2L} W_i^{(c)} \{\mathcal{Y}_i - \bar{Y}\}\{Y_i - \bar{Y}\}^T$$

The UKF algorithm is computed as follows:

- Initialize

$$\hat{X}_0 = \boldsymbol{E}[X_0]\boldsymbol{P}_0 = \boldsymbol{E}[(X_0 - \hat{X}_0)(X_0 - \hat{X}_0)^T]$$

- Calculate sigma points for $k \in \{1, ..., \infty\}$

$$\mathcal{X}_{k-1|k-1} = \begin{bmatrix} \hat{X}_{k-1|k-1} & \hat{X}_{k-1|k-1} \pm \sqrt{(L+\lambda)\boldsymbol{P}^a_{k-1|k-1}} \end{bmatrix}$$

- Time update

$$\begin{aligned}
\mathcal{X}_{k|k-1} &= F[\mathcal{X}_{k-1}, \mathcal{X}^v_{k-1}] \\
\hat{X}_{k|k-1} &= \sum_i^{2L} W_i^{(m)} \mathcal{X}_{i,k|k-1} \\
P_{k|k-1} &= \sum_i^{2L} W_i^{(c)} [\mathcal{X}_{i,k|k-1} - \hat{X}_{k|k-1}][\mathcal{X}_{i,k|k-1} - \hat{X}_{k|k-1}]^T \\
\mathcal{Y}_{k|k-1} &= H[\mathcal{X}_{k-1}, \mathcal{X}^n_{k-1}] \\
\hat{Y}_{k|k-1} &= \sum_i^{2L} W_i^{(m)} \mathcal{Y}_{i,k|k-1}
\end{aligned}$$

- Measurement update

$$
\begin{aligned}
P_{\tilde{y}_k\tilde{y}_k} &= \sum_{i}^{2L} W_i^{(c)}[\mathcal{Y}_{i,k|k-1} - \hat{Y}_{k|k-1}][\mathcal{Y}_{i,k|k-1} - \hat{Y}_{k|k-1}]^T \\
P_{x_k y_k} &= \sum_{i}^{2L} W_i^{(c)}[\mathcal{X}_{i,k|k-1} - \hat{X}_{k|k-1}][\mathcal{Y}_{i,k|k-1} - \hat{Y}_{k|k-1}]^T \\
\mathcal{K} &= P_{x_k y_k} P_{\tilde{y}_k\tilde{y}_k}^{-1} \\
\hat{X}_k &= \hat{X}_{k|k-1} + \mathcal{K}(Y_k - \hat{Y}_{k|k-1}) \\
P_k &= P_{k|k-1} - \mathcal{K} P_{\tilde{y}_k\tilde{y}_k} \mathcal{K}^T
\end{aligned}
$$

3.3. Adaptive Control With Estimated Parameters

To estimate parameters a, b and c in eq.(13) for designing adaptive controller, the derived model is remodeled as the nonlinear differential system equation by letting $x_1 = \omega, x_2 = a, x_3 = b, x_4 = c$ as states. The continuous-discrete stochastic nonlinear equation for processing model and measuring model is obtained as follows:

$$
\begin{aligned}
\begin{bmatrix} \dot{x}_1 \\ \dot{x}_2 \\ \dot{x}_3 \\ \dot{x}_4 \end{bmatrix} &= \begin{bmatrix} x_1 x_2 + x_3 u - x_4 \\ 0 \\ 0 \\ 0 \end{bmatrix} + \sqrt{Q_c} v(t) \\
[y]_k &= \begin{bmatrix} 1 & 0 & 0 & 0 \end{bmatrix} \begin{bmatrix} x_1 \\ x_2 \\ x_3 \\ x_4 \end{bmatrix}_k + \sqrt{R} w_k.
\end{aligned}
\tag{14}
$$

Then, the processing model and measurement model in eq.(14) are discretized as follows:

$$
\begin{aligned}
\begin{bmatrix} x_1 \\ x_2 \\ x_3 \\ x_4 \end{bmatrix}_k &= \begin{bmatrix} x_1 \\ x_2 \\ x_3 \\ x_4 \end{bmatrix}_{k-1} + T_s \begin{bmatrix} x_1 x_2 + x_3 u - x_4 \\ 0 \\ 0 \\ 0 \end{bmatrix}_{k-1} + \sqrt{T_s Q_c} v_{k-1} \\
[y]_k &= \begin{bmatrix} 1 & 0 & 0 & 0 \end{bmatrix} \begin{bmatrix} x_1 \\ x_2 \\ x_3 \\ x_4 \end{bmatrix}_k + \sqrt{R} w_k.
\end{aligned}
\tag{15}
$$

To estimate lumped parameters for designing the adaptive controller, the UKF algorithm is placed after the angular velocity signal in Fig. 2 . Then, the adaptive rotational dynamic controller is obtained by replacing parameter a, b and c with the estimated states x_2, x_3 and x_4 as shown in Fig. 3. Since the estimated states change according to UAV motion, the controller gains and compensated values which are obtained by the above estimated values also changes accordingly. This make the controller adaptive to the UAV motion. The first order filter block $\dot{x} = \frac{1}{\lambda}(x + \hat{x})$ as studied in [40] is used to smooth the estimated parameters to tune the controller gains k_p and k_i and compensated values for controlling . Here unlike the controller in Fig. 2, the real dynamic model of angular velocity eq.(10) is preferred to the derived model. The output angular velocity ω is discretized into a measuring model to use as input signal adding to the output controlling signal u for the UKF block.The components of estimated parameter $\hat{x}$, the estimated angular velocity $\hat{x}_1$ is used to feedback the desired angular velocity ω_d, the estimated parameters $\hat{x}_2, \hat{x}_3$ and $\hat{x}_4$ are used as input signal for the filter.

The effectiveness of the designed controller is confirmed by simulating results in Fig. 4, in which the estimated random parameters are plotted against the filtered parameters. The following parameters are used the simulation: $\mathbf{J} = [0.5 - 0.1 - 0.15; -0.10.5 - 0.2; -0.15 - 0.20.5]^\top, Qc = 1e-6 * diag([1; 0.1; 0.1; 0.1]); R = 1e-4$, desired angular velocity is sine wave $\omega_d = 1.8sin(4t)(rad/s)$, the two other moments $u_y = sin(5t)(N.m), u_z = sin(3t)(N.m), \xi = 1$, and $\omega_n = 2\times\pi\times5(rad/s)$. After 4 second, the estimated values $\hat{x}_2, \hat{x}_3, \hat{x}_4, \omega_{est}$ are stably walking in the bounded finite interval while the filtered values are smoothly following those estimated values. The error between desired and estimated angular velocity is very decent, $e_\omega \approx 0.008(rad/s)$.

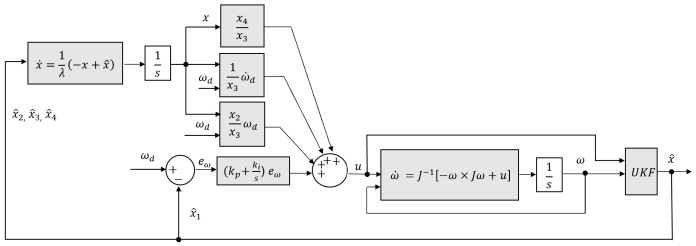

Fig. 3. Adaptive controller with estimated parameters

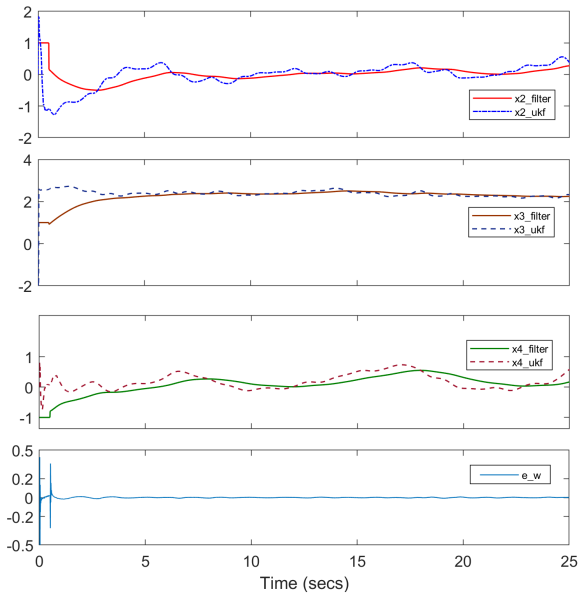

Fig. 4. Estimated parameters $\hat{x}_2, \hat{x}_3, \hat{x}_4, \omega$

4. Controller System of Quadcopter

The entire controller of quadcopter consists five blocks, namely, desired trajectory controller, attitude-thrust controller, angular rate controller, adaptive controller, and translational kinematic, which are illustrated in Fig. 5. Each block controller consists of controlling techniques which will be described in the following subsections. The adaptive controller block consists of 3 three adaptive controllers as shown in Fig. 3 for controlling rotational motion about x, y and z axes simultaneously.

4.1. Desired Trajectory Controller

The desired trajectory controller block is designed to generate desired trajectory $X_d = (x_d, y_d, z_d)^\top$ and desired yaw angle ψ_d as study in [41] and [42]. The desired trajectory X_d can be a line, circular,

spiral paths in plane or in space as required by operation. It can be adjusted by a first order filter or second order filter so that the controller can follow the paths. The desired yaw angle ψ_d can be defined according to the requirement of the trajectory. It will be used as the input signals for the attitude and thrust controller block. In this study, as illustrated in Fig. 6, the yaw angle ψ_d is determined as follows:

$$\psi_d = tan^{-1}\left(\frac{y_i - y_{i-1}}{x_i - x_{i-1}}\right),$$

where (x_{i-1}, y_{i-1}) is the current position, (x_i, y_i) is the next position of the UAV path in the initial frame [43]-[45].

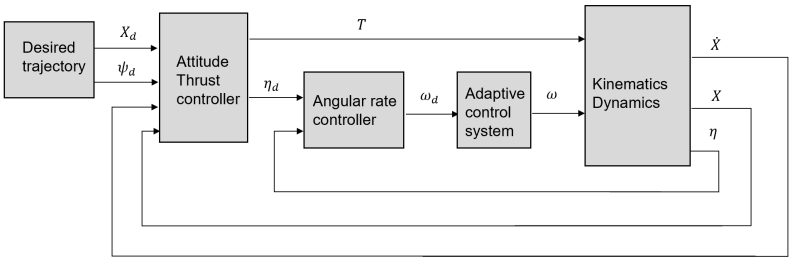

Fig. 5. Quadcopter controller

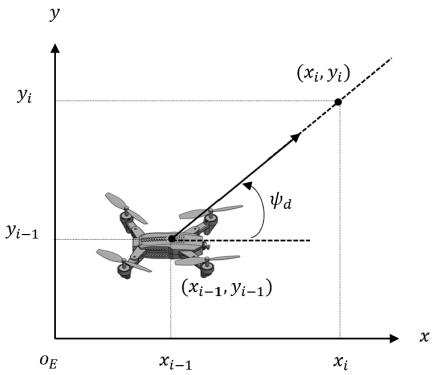

Fig. 6. Desired yaw angle ψ_d

.

4.2. Attitude and Thrust Controller

The attitude and thrust controller is built as shown in Fig. 7. According to Newton's second law of motion and the transformation of matrix eq.(2), the translational motion of UAV with mass m, which is moved by force $\mathbf{F}_t = F_t(0,0,1)^\top$ in body frame, can be expressed in terms of acceleration $\ddot{\mathbf{X}}_d = (\ddot{x}_d, \ddot{y}_d, \ddot{z}_d)^\top$ and Euler angle $\eta_d = (\phi_d, \theta_d, \psi_d)^\top$ in inertial frame as follows:

$$m\ddot{\mathbf{X}}_d = \mathcal{R}_b^v \mathbf{F}_t + m\begin{bmatrix}0\\0\\g\end{bmatrix}$$

$$m\begin{bmatrix}\ddot{x}_d\\ \ddot{y}_d\\ \ddot{z}_d\end{bmatrix} = -F_t\begin{bmatrix}c_{\phi_d}s_{\theta_d}c_{\psi_d} + s_{\phi_d}s_{\psi_d}\\ c_{\phi_d}s_{\theta_d}s_{\psi_d} - s_{\phi_d}c_{\psi_d}\\ c_{\phi_d}c_{\theta_d}\end{bmatrix} + m\begin{bmatrix}0\\0\\g\end{bmatrix}. \quad (16)$$

To solve for ϕ_d and θ_d, the equation eq.(16) is arranged as following expression,

$$\ddot{x}_d = \frac{-F_t}{m}(c_{\phi_d} s_{\theta_d} c_{\psi_d} + s_{\phi_d} s_{\psi_d}) \tag{16-a}$$

$$\ddot{y}_d = \frac{-F_t}{m}(c_{\phi_d} s_{\theta_d} s_{\psi_d} - s_{\phi_d} c_{\psi_d}) \tag{16-b}$$

$$g - \ddot{z}_d = \frac{-F_t}{m} c_{\phi_d} c_{\theta_d}. \tag{16-c}$$

As studied in[43]-[48], the desired roll ϕ_d and pitch θ_d angles are obtained by performing below calculating :

$$\frac{-(16\text{-a})c_{\psi_d} - (16\text{-b})s_{\psi_d}}{(16\text{-c})} \Rightarrow \theta_d = tan^{-1}\left(\frac{\ddot{x}_d c_{\psi_d} - \ddot{y}_d s_{\psi_d}}{g - \ddot{z}_d}\right)$$

$$\frac{-(16\text{-a})s_{\psi_d} + (16\text{-b})c_{\psi_d}}{(16\text{-c})} \Rightarrow \phi_d = tan^{-1}\left(\frac{\ddot{x}_d s_{\psi_d} - \ddot{y}_d c_{\psi_d}}{g - \ddot{z}_d} c_{\theta_d}\right).$$

From the third row of eq.(16), the magnitude of the thrust is $F_t = m(-\ddot{z}_d + g)/(c_{\phi_d} c_{\theta_d})$.

To control the thrust, this study defines PD controller by adding it into acceleration $\ddot{z}_d$ to control the total thrust as following,

$$T = m(-\ddot{z}_d - k_{pt} e_z - k_{dt} \dot{e}_z + g)/(c_{\phi_d} c_{\theta_d}) \tag{17}$$

where k_{pt}, k_{dt} are PD controller gains that can be tuned as described in study [49], $e_z = z_d - z$ is the altitude error, and $\dot{e}_z = \dot{z}_d - \dot{z}$ is the time derivative of the error e_z. The desired acceleration $\ddot{z}_d$, the attitude error e_z and the derivative of attitude error $\dot{e}_z$ in the thrust controller eq.(17), will be computed in the following attitude and thrust controller block. As shown in the block diagram in Fig. 7, the attitude and thrust controller are composed of a position controller and a velocity controller in Cascade controlling method.

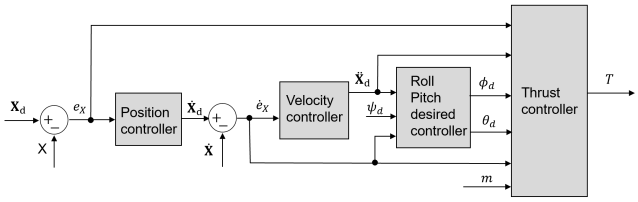

Fig. 7. Attitude and Thrust controller

As study in [50]-[52], PD controller is defined to control desired position X_d with output signal as velocity $\dot{X}_d$. Then, the output velocity $\dot{X}_d$ is used as input signal to another PD controller to control the velocity $\dot{X}_d$ with the output signal as the desired acceleration $\ddot{X}_d$. The attitude error e_z and the derivative of attitude error $\dot{e}_z$ are also obtained in the position controller and velocity controller.

4.3. Angular Rate Controller

The angular rate controller is built as shown in Fig. 8. The yaw rate is defined by P controller and it is compensated with the time derivative of desired yaw angle.The roll rate and pitch rate are also defined by the PD controllers. Finally, $\phi_d, \theta_d, \dot{\phi}_d, \dot{\theta}_d, \dot{\psi}_d$ are determined. Then, the desired angular velocity or desired body rate is calculated by using kinematic equation of motion in eq.(4) as follows:

$$\begin{bmatrix} \omega_{x_d} \\ \omega_{y_d} \\ \omega_{z_d} \end{bmatrix} = \begin{bmatrix} p_d \\ q_d \\ r_d \end{bmatrix} = \begin{bmatrix} 1 & 0 & -\sin\theta_d \\ 0 & \cos\phi_d & \sin\phi_d \cos\theta_d \\ 0 & -\sin\phi_d & \cos\phi_d \cos\theta_d \end{bmatrix} \begin{bmatrix} \dot{\phi}_d \\ \dot{\theta}_d \\ \dot{\psi}_d \end{bmatrix}.$$

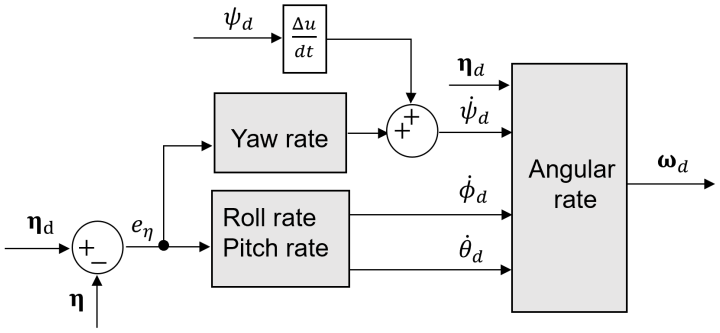

Fig. 8. Angular rate controller

4.4. Kinematics and Dynamics

Since drag $\mathbf{D}$ is always presenting in UAV translational motion, the total external force acting on UAV is obtained as:

$$\mathbf{F}_b = m\mathbf{g}_b + \mathbf{F}_d - \mathbf{T}.$$

From the rotational transformation matrix $\mathcal{R}_v^b(\phi, \theta, \psi)$ in eq.(1), the dynamics model eq.(7) in body frame becomes

$$m\mathbf{g}_b + \mathbf{F_d} - \mathbf{T} = m\dot{\mathbf{V}} + \boldsymbol{\omega} \times m\mathbf{V}.$$

Expressing this equation in terms of acceleration $\dot{\mathbf{V}}$ gives

$$\dot{\mathbf{V}} = -\boldsymbol{\omega} \times \mathbf{V} + \mathbf{g}_b + \frac{1}{m}(\mathbf{F}_d - \mathbf{T})$$

$$\begin{bmatrix} \dot{u} \\ \dot{v} \\ \dot{w} \end{bmatrix} = \begin{bmatrix} 0 & r & -q \\ -r & 0 & p \\ q & -p & 0 \end{bmatrix} \begin{bmatrix} u \\ v \\ w \end{bmatrix} + g \begin{bmatrix} -s_\theta \\ s_\phi c_\theta \\ c_\phi c_\theta \end{bmatrix} + \frac{1}{m} \left(\begin{bmatrix} D_x & 0 & 0 \\ 0 & D_y & 0 \\ 0 & 0 & D_z \end{bmatrix} \begin{bmatrix} u \\ v \\ w \end{bmatrix} - \begin{bmatrix} 0 \\ 0 \\ T \end{bmatrix} \right). \quad (18)$$

As observing eq.(18), the total acceleration is the sum of gyroscopic, gravitational, drag, and mass acceleration on UAV. To compute the states $\mathbf{X} = (x, y, z)^\top$ of UAV in initial frame, the block diagram of translational dynamics is obtained and arranged as Fig. 9.

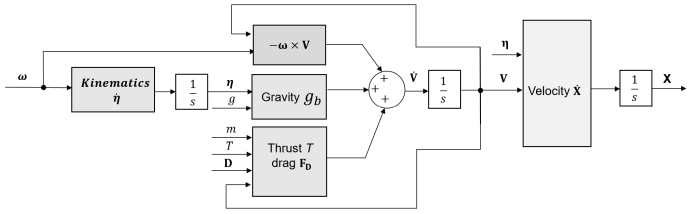

Fig. 9. Kinematics and Dynamics

The Euler angle state $\boldsymbol{\eta} = (\phi, \theta, \psi)^\top$ is obtained by using transformation matrix eq.(5) with body rate $\boldsymbol{\omega} = (p, q, r)^\top$ as the input, and adding the results with the integrator $\frac{1}{s}$ with zero initial condition. The velocity state $\mathbf{V} = (u, v, w)^\top$ in body frame is obtained by implementing eq.(18) and adding results with integrator $\frac{1}{s}$ with zero initial condition. The position state $\mathbf{X} = (x, y, z)^\top$ is obtained by

using kinematic relationship eq.(3) on $\mathbf{V} = (u, v, w)^\top$ to become $\dot{\mathbf{X}} = (\dot{x}, \dot{y}, \dot{z})^\top$ in the initial frame and adding results with integrator $\frac{1}{s}$ with zero initial condition. Then, the state $\mathbf{X} = (x, y, z)^\top$ is used to feedback the desired path $\mathbf{X}_d = (x_d, y_d, z_d)^\top$ in the altitude thrust controller in Fig. 7.

5. Simulation and Results

In the quadcopter controller system in Fig. 5, the rotational adaptive controller plays a core controller for trajectory tracking. It is designed by considering relevant uncertainties such as inertia, angular rate, aerodynamic drag, gyroscopic effect in the rotational dynamics as lamped parameters to be estimated by UKF during the UAV operation for designing controller as illustrated in Fig. 3. To verify the effectiveness of the proposed controller, the circular trajectory and square trajectory are used for simulation. The results of trajectory tracking, estimated parameters, and angular velocity are depicted and observed. The controller gains in the controller blocks used in the simulation are listed in Table 2. The parameters such as translational motion drag, model noise used in the simulation are listed in Table 3.

Table 2. Controller gains used in simulation

Name of controllers	**Description**		
	Proportional gain K_p	Integral gain K_i	Derivative gain K_d
Position	0.75	0	0.02
Velocity	0.85	0.02	0
Thrust	11.52	0	4.8
Yaw rate	1	0	0
Roll rate	6	0	0.2
Pitch rate	6	0	0.2
Adaptive	$\frac{2\xi\omega_n - a}{b}$	$\frac{\omega_n^2}{b}$	0

Table 3. Constant parameters used in simulation

Name of parameters	**Description**		
	Symbol	Value	Units
Drag coefficient	$\mathbf{D}$	$(2.5, 2.5, 2.3)^\top$	$N.s/s^2$
Gravitational acceleration	g	9.81	m/s^2
Total mass of UAV	m	76	Kg
Sampling time	T_s	0.02	s
Natural frequency	ω_n	6π	rad/s
Damping ratio	ξ	1	-
Filter constant	λ	2	-
Model noise	Qc	$1e-3 * diag([10; 1; 1; 1])$	-
Measurement noise	R	$1e-4 * diag([2; 2])$	-

5.1. Circular Trajectory

For the circular trajectory, the following desired path is chosen for UAV to track for 25 seconds in the simulation,

$$x_d(t) = 8cos(\frac{\pi}{8})t \ \ (m)$$
$$y_d(t) = 8cos(\frac{\pi}{8})t \ \ (m)$$
$$z_d(t) = -10 \ \ (m).$$

Results of the circular trajectory tracking are depicted in Fig. 10. The designed controller allows the UAV to successfully track the desired path from 10 seconds. The steady state errors for x axis and

y axis are less than 0.04 m, the altitude state starts to reach the desired state from 2.5 seconds while the steady state errors is less than 0.02 m. The altitude error is very small, enough to keep the UAV stable with low vibration.

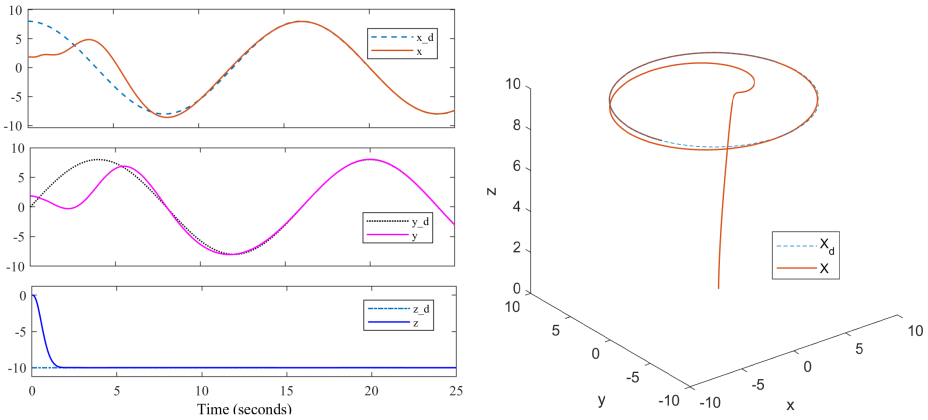

(a) Circular trajectory in plane against times **(b)** Trajectory in space

Fig. 10. Circular in space view

Results of parameter estimation for circular trajectory are depicted in Fig. 11 (a), (b) and (c), in which the estimated random parameters are plotted against the filtered ones. At less than 5 seconds, the estimated parameters have very big variation due to the nature of UKF algorithm which does not work well for first short period. This variation is smoothed by the first order filter for the controller to work properly. After that period, the estimated parameters are very smooth and almost constant as the UKF algorithm works well.

The results of the angular velocity estimation for circular trajectory are depicted in Fig. 11 (d), in which the angular velocities of the UAV are plotted against the estimated ones. At less than 5 seconds, the estimated parameters have very big variation due to the nature of UKF algorithm which does not work well for first short period. After that period, the estimated angular velocities reach the angular velocities of the UAV and almost constant as the UKF algorithm works well. The previously mentioned variation of the angular velocity is not so significant that makes sense of the study to use the concepts of the random walking parameters.

5.2. Square Trajectory

For the square trajectory, the following desired path is chosen for UAV to track during 40 seconds in the simulation.

$$x(t) = \begin{cases} 0 & t < 10 \\ -10 + t \ \ (m) & 10 \leq t < 20 \\ 10 \ \ (m) & 20 \leq t < 30 \\ 40 - t \ \ (m) & 30 \leq t < 40 \end{cases}$$

$$y(t) = \begin{cases} t \ \ (m) & t < 10 \\ 10 \ \ (m) & 10 \leq t < 20 \\ 30 - t \ \ (m) & 20 \leq t < 30 \\ 0 \ \ (m) & 30 \leq t < 40 \end{cases}$$

$$z(t) = -8 \ \ (m)$$

The results of the square trajectory are depicted in Fig. 12. The designed controller allows UAV

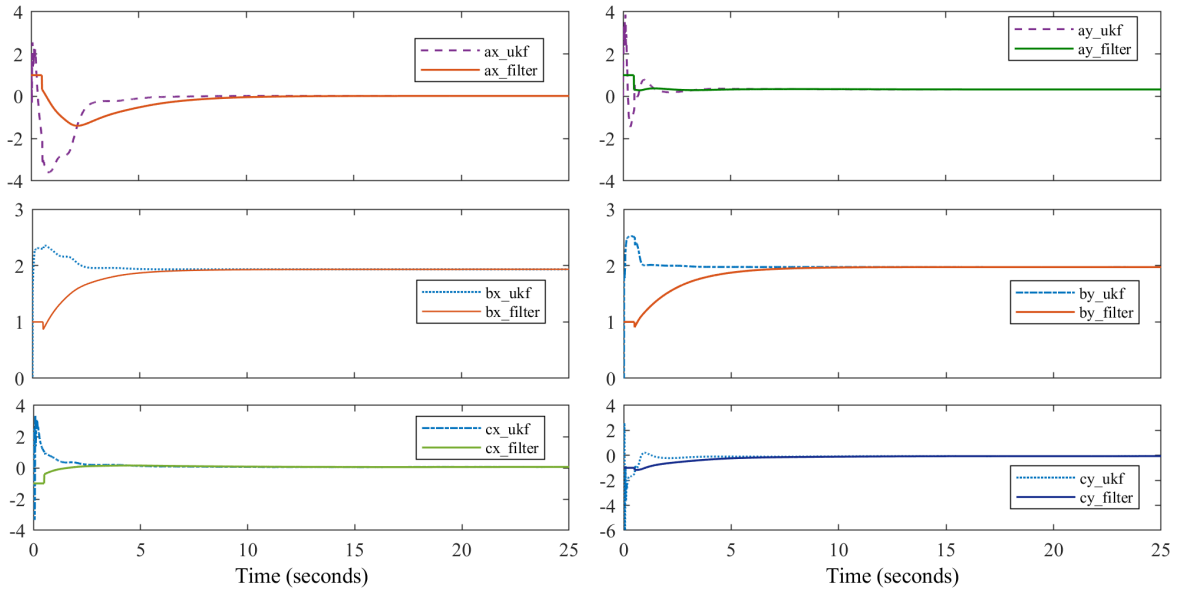

(a) a_x, b_x, c_x estimation

(b) a_y, b_y, c_y estimation

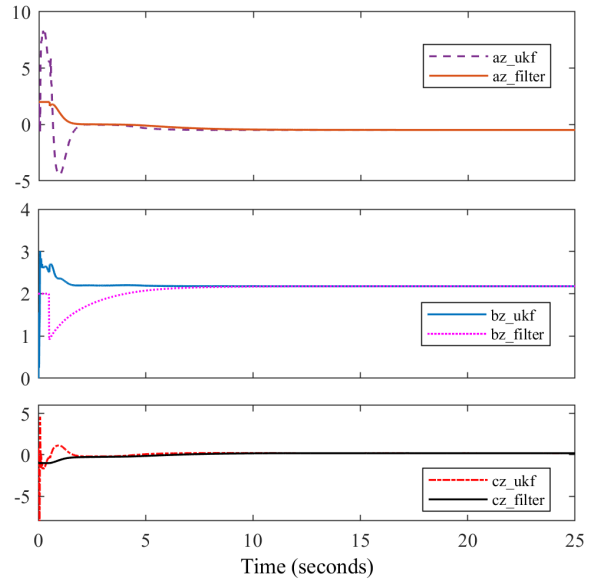

(c) a_z, b_z, c_z estimation

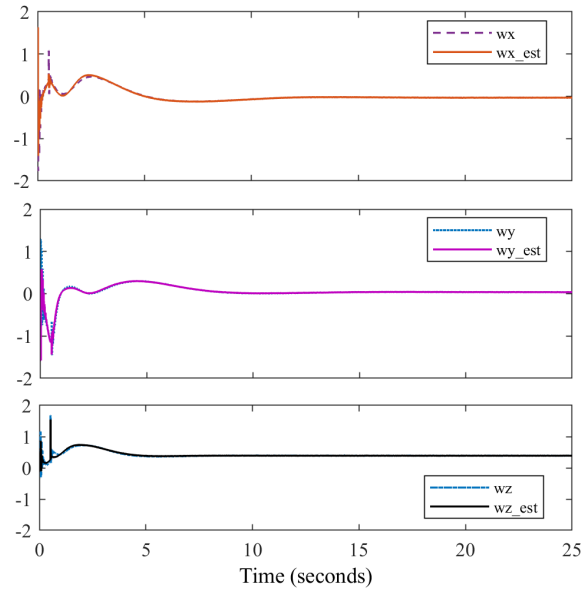

(d) Angular velocity

Fig. 11. Estimated random parameters for circular trajectory

to successfully track the desired path from 5 seconds. Although trajectory path in horizontal plane changes $\pi/2$ radians, which causes overshoot, the steady state errors for x axis and y axis are less than 0.05 m and the altitude state starts to reach the desired state from 2.5 seconds with the steady state errors of less than 0.02 m. The altitude error is very small. This keeps the UAV stable with low vibration.

The results of the parameter estimation for square trajectory are depicted in Fig. 13(a), (b) and (c), in which the estimated random parameters are plotted against the filtered ones. At less than 5 seconds, the estimated parameters have very big variation due to the nature of UKF algorithm which does not work well for first short period of time. This variation is smoothed by the filter for the controller to work properly. After that period, the estimated parameters a and c are very smooth,

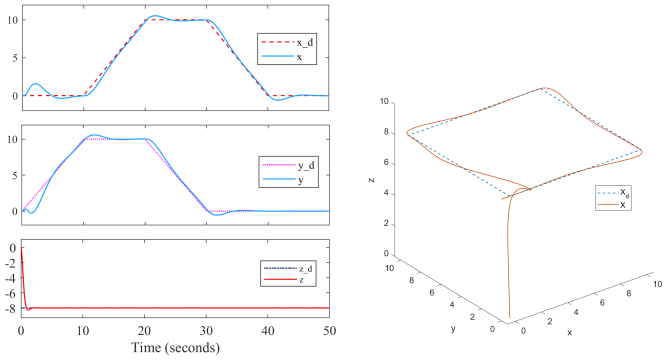

(a) Square trajectory in plane against times **(b)** Trajectory in space

Fig. 12. Square trajectory in space view

and almost constant as UKF algorithm works well. The estimate parameter b keeps changing slightly in correspond to the changing of path angle, and it is smoothed by the filter. The angular velocity estimation for square trajectory are depicted in Fig. 13(d), in which the angular velocities of the UAV are plotted gain the estimated ones. At less than 2 seconds, the estimate parameters have very big variation due to the nature of UKF algorithm which does not work well for first short period. After that period the estimated angular velocities reach the actual angular velocities of the UAV and almost constant, except at the change of trajectory direction by $\pi/2$ radians. This consequence corresponds with the results of the trajectory in Fig. 12. The previously mentioned variation of the angular velocity is not so significant that makes sense of the study to use the concepts of the random walking parameters.

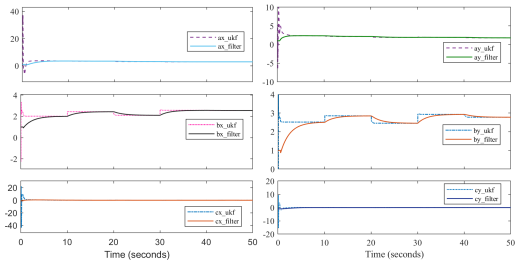

(a) a_x, b_x, c_x estimation **(b)** a_y, b_y, c_y estimation

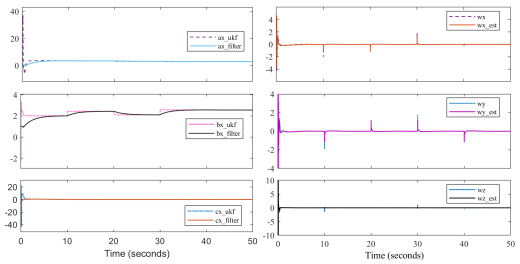

(c) a_z, b_z, c_z estimation **(d)** Angular velocity

Fig. 13. Estimated random parameters for square trajectory

6. Conclusion and future work

In this study, the trajectory tracking controller of UAV is proposed. The rotational dynamic motion is derived and simplified into first order differential equation where their coefficients are the lumped parameters of wind disturbance, angular rate, inertia or gyroscopic effect. Then, the rotational controller is designed to control the simplified angular velocity.The simplified model is remodeled into processing and measuring model for estimating the lumped parameters which are used for tuning PI gain and compensating signal in the rotational dynamic controller to be adaptive. Also, in the adaptive controller, the rotational model of UAV is used and UKF algorithm is implemented to estimate those lumped parameters which are random walking which are smoothed by the first order filter in three axis rotations simultaneously. The whole system controller of quadcopter is designed by adding desired trajectory controller, attitude-thrust controller, and angular rate controller to the adaptive controller. The circular trajectory path and square trajectory paths are used to simulate the controller to assess the performance of controller on tracking, variations of the estimated random parameters and angular velocity of UAV. From the results of the simulation, it is observed that the controllers are performing well for both paths. The states of UAV reach the desired state about 10 seconds on both paths with very small errors. The estimated random parameters at first 3 seconds inhibits high variation due to UKF working behaviors. This is smoothed by the first order filter. After that period, the estimated parameters are not much walking away from the actual ones which almost remain constant. The variation of estimated parameters and the angular velocities behave correspondingly to the changing of the trajectory path. These behaviors allow the adaptive controller to works efficiently.

For the future expansion, the adaptive rotational dynamic controller will be first verified by experiment with an apparatus which is designed for UAV rotational motion by using Pixhawk 4 controller. Then the real experiments for trajectory tracking will be conducted to assess the performance of the controller and state estimation.

Author Contribution: All authors contributed equally to the main contributor to this paper. All authors read and approved the final paper.

Funding: Research was funded by Asian Office of Aerospace Research and Development(AOARD), grant number FA2386-21-1-4009.

Conflicts of Interest: The authors declare no conflict of interest. The funders had no role in designing study, interpreting data, writing the manuscript, nor publishing the results.

References

[1] F. Ahmed, J. C. Keshari, and Pankaj Singh Yadav, "Recent Advances in Unmanned Aerial Vehicles: A Review," *Arabian Journal for Science and Engineering*, vol. 47, pp. 7963–7984, 2022, https://doi.org/10.1007/s13369-022-06738-0.

[2] J. Kim, S. A. Gadsden and S. A. Wilkerson, "A Comprehensive Survey of Control Strategies for Autonomous Quadrotors," in *Canadian Journal of Electrical and Computer Engineering*, vol. 43, no. 1, pp. 3-16, 2020, https://doi.org/10.1109/CJECE.2019.2920938.

[3] S. A. H. Mohsan, N. Q. H. Othman, Y. Li, M. H. Alsharif and M. A. Khan, "Unmanned aerial vehicles (UAVs): practical aspects, applications, open challenges, security issues, and future trends," *Intelligent Service Robotics*, vol. 16, pp.109–137, 2023, https://doi.org/10.1007/s11370-022-00452-4.

[4] N. Mohamed, J. Al-Jaroodi, I. Jawhar, A. Idries and F. Mohammed, "Unmanned aerial vehicles applications in future smart cities," *Technological Forecasting and Social Change*, vol. 153, 2020, https://doi.org/10.1016/j.techfore.2018.05.004.

[5] M. Idrissi, M. Salami, and F. Annaz, "A Review of Quadrotor Unmanned Aerial Vehicles: Applications, Architectural Design and Control Algorithms," *Journal of Intelligent & Robotic Systems*, vol. 104, no. 22, 2022, https://doi.org/10.1007/s10846-021-01527-7.

[6] M. Hassanalian and A. Abdelkefi, "Classifications, applications, and design challenges of drones: A review," *Progress in Aerospace Sciences*, vol. 91, pp. 99-131, 2017, https://doi.org/10.1016/j.paerosci.2017.04.003.

[7] H. Shraim, A. Awada and R. Youness, "A survey on quadrotors: Configurations, modeling and identification, control, collision avoidance, fault diagnosis and tolerant control," in *IEEE Aerospace and Electronic Systems Magazine*, vol. 33, no. 7, pp. 14-33, 2018, https://doi.org/10.1109/MAES.2018.160246.

[8] M. Maaruf, M. S. Mahmoud and A. Ma'arif, "A Survey of Control Methods for Quadrotor UAV," *International Journal of Robotics and Control Systems*, vol. 2, no. 4, pp. 652-665, 2022, https://doi.org/10.31763/ijrcs.v2i4.743.

[9] S. Abdelhay and A. Zakriti, "Modeling of a Quadcopter Trajectory Tracking System Using PID Controller," *Procedia Manufacturing,* vol. 32, pp. 564-571, 2019, https://doi.org/10.1016/j.promfg.2019.02.253.

[10] R. Mahony, V. Kumar and P. Corke, "Multirotor Aerial Vehicles: Modeling, Estimation, and Control of Quadrotor," in *IEEE Robotics & Automation Magazine*, vol. 19, no. 3, pp. 20-32, 2012, https://doi.org/10.1109/MRA.2012.2206474.

[11] I. S. Leal, C. Abeykoon, and Y. S. Perera, "Design, Simulation, Analysis and Optimization of PID and Fuzzy Based Control Systems for a Quadcopter," *Electronics*, vol. 10, no. 18, 2021, https://doi.org/10.3390/electronics10182218.

[12] O. Doukhi, A. Razzaq Fayjie, and D. J. Lee, "Intelligent Controller Design for Quad-Rotor Stabilization in Presence of Parameter Variations," *Journal of Advanced Transportation*, vol. 2017, 2017, https://doi.org/10.1155/2017/4683912.

[13] A. A. Najm and I. K. Ibraheem, "Nonlinear PID controller design for a 6-DOF UAV quadrotor system," *International Journal of Engineering Science and Technology*, vol. 22, pp. 1087-1097, 2019, https://doi.org/10.1016/j.jestch.2019.02.005.

[14] A. Abdulkareem, V. Oguntosin, O. M. Popoola, and A. A. Idowu, "Modeling and Nonlinear Control of a Quadcopter for Stabilization and Trajectory Tracking," *Journal of Engineering*, vol. 2022, pp. 1–19, 2022, https://doi.org/10.1155/2022/2449901.

[15] Z. Cai, S. Zhang and X. Jing, "Model Predictive Controller for Quadcopter Trajectory Tracking Based on Feedback Linearization," in *IEEE Access*, vol. 9, pp. 162909-162918, 2021, https://doi.org/10.1109/ACCESS.2021.3134009.

[16] J. C. Pereira, V. J. S. Leite, and G. V. Raffo, "Nonlinear Model Predictive Control on SE(3) for Quadrotor Aggressive Maneuvers," *Journal of robotic and Intelligent system*, vol. 62, no. 101, 2021, https://doi.org/10.1007/s10846-021-01310-8.

[17] A. T. Nguyen, N. X. Mung, and S. K. Hong, "Quadcopter Adaptive Trajectory Tracking Control: A New Approach via Backstepping Technique," *Applied Sciences*, vol. 9, no. 18, 2019, https://doi.org/10.3390/app9183873.

[18] A. Noordin, M. A. Mohd Basri, and Z. Mohamed, "Adaptive PID Control via Sliding Mode for Position Tracking of Quadrotor MAV: Simulation and Real-Time Experiment Evaluation," *Aerospace*, vol. 10, no. 6, 2023, https://doi.org/10.3390/aerospace10060512.

[19] M. Vahdanipour, and M. Khodabandeh, "Adaptive fractional order sliding mode control for a quadrotor with a varying load," *Aerospace Science and Technology*, vol. 86, pp. 737-747, 2019, https://doi.org/10.1016/j.ast.2019.01.053.

[20] A. Saibi, R. Boushaki, and H. Belaidi, "Backstepping Control of Drone," *Engineering Proceedings*, vol. 14, no. 1, 2022, https://doi.org/10.3390/engproc2022014004.

[21] Z. Li, X. Ma and Y. Li, "Robust trajectory tracking control for a quadrotor subject to disturbances and model uncertainties," *International Journal of Systems Science*, vol. 51, no. 5, pp. 839-851, 2020, https://doi.org/10.1080/00207721.2020.1746430.

[22] A. Daadi, H. Boulebtinai, S. H. Derrouaoui and F. Boudjema, "Sliding Mode Controller Based on the Sliding Mode Observer for a QBall 2+ Quadcopter with Experimental Validation," *International Journal of Robotics and Control Systems*, vol. 2, no. 2, pp. 332-356, 2022, https://doi.org/10.31763/ijrcs.v2i2.693.

[23] H. Coppejans and H. Myburgh, "A Primer on Autonomous Aerial Vehicle Design," *Sensors*, vol. 15, no. 12, pp. 30033–30061, 2015, https://doi.org/10.3390/s151229785.

[24] M. Karahan, M. Inal and C. Kasnakoglu, "Fault Tolerant Super Twisting Sliding Mode Control of a Quadrotor UAV Using Control Allocation," *International Journal of Robotics and Control Systems*, vol. 3, no. 2, pp. 270-285, 2023, https://doi.org/10.31763/ijrcs.v3i2.994.

[25] E. Morelli and V. Klein, "Aircraft System Identification: Theory And Practice," *AIAA (American Institute of Aeronautics & Astronautics),* pp. 27-38, 2016, https://doi.org/10.2514/4.861505.

[26] A. T. E. Fraire, A. E. D. López, R. P. P. Morado, and J. A. S. Esqueda, "Design of Control Laws and State Observers for Fixed-Wing UAVs: Simulation and Experimental Approaches," *Elsevier*, pp. 24-30, 2023, https://doi.org/10.1016/C2021-0-02985-0.

[27] M. N. Shauqee, P. Rajendran and N. M. Suhadis, "An effective proportional-double derivative-linear quadratic regulator controller for quadcopter attitude and altitude control," *Automatika*, vol. 62, no. 3-4, pp. 415–433, 2021, https://doi.org/10.1080/00051144.2021.1981527.

[28] R. W. Beard and T. W. McLain, "Small Unmanned Aircraft: Theory and Practice," *Princeton University Press 2012*, pp. 8-28, 2023, https://doi.org/10.1515/9781400840601.

[29] S. Srey, V. Chhour and S. Srang, "Lumped Parameter Estimation of a Low Cost DC Motor for Position Controller Design," *2021 International Conference on Advanced Mechatronics, Intelligent Manufacture and Industrial Automation*, pp. 1-6, 2021, http://doi.org/10.1109/ICAMIMIA54022.2021.9807810.

[30] S. Yean, T. Peou, B. Sethy and S. Srang, "PD Controller and Dynamic Compensation Design for a DC Motor based on Estimated Parameters," *2021 International Conference on Advanced Mechatronics, Intelligent Manufacture and Industrial Automation*, pp. 7-12, 2021, http://doi.org/10.1109/ICAMIMIA54022.2021.9807796.

[31] N. S. Nise, "Control Systems Engineering," *John Wiley & Sons,* 8^{th} *edition*, pp. 160-180, 2019, https://bit.ly/4bbwAal.

[32] M. A. Haidekker, "Chapter 3 - Solving Differential Equations in the Laplace Domain," *Linear Feedback Controls*, pp. 27–56, 2013, https://doi.org/10.1016/B978-0-12-405875-0.00003-6.

[33] M. A. Tahir, I. Mir, and T. U. Islam, "Control Algorithms, Kalman Estimation and Near Actual Simulation for UAVs: State of Art Perspective," *Drones*, vol. 7, no. 6, 2023, https://doi.org/10.3390/drones7060339.

[34] H. G. de Marina, F. J. Pereda, J. M. Giron-Sierra and F. Espinosa, "UAV Attitude Estimation Using Unscented Kalman Filter and TRIAD," in *IEEE Transactions on Industrial Electronics*, vol. 59, no. 11, pp. 4465-4474, 2012, https://doi.org/10.1109/TIE.2011.2163913.

[35] J. L. Crassidis and F. L. Markley, "Unscented Filtering for Spacecraft Attitude Estimation," *Journal of Guidance, Control, and Dynamics*, vol. 26, no. 4, pp. 536-542, 2012, https://doi.org/10.2514/2.5102.

[36] E. A. Wan and R. Van Der Merwe, "The unscented Kalman filter for nonlinear estimation," *Proceedings of the IEEE 2000 Adaptive Systems for Signal Processing, Communications, and Control Symposium*, pp. 153-158, 2000, https://doi.org/10.1109/ASSPCC.2000.882463.

[37] C. Urrea, and R. Agramonte, "Kalman Filter: Historical Overview and Review of Its Use in Robotics 60 Years after Its Creation," *Journal of Sensors*, vol. 2021, 2021, https://doi.org/10.1155/2021/9674015.

[38] R. Zanetti and K. J. DeMars, "Fully Multiplicative Unscented Kalman Filter for Attitude Estimation," *Journal of Guidance, Control, and Dynamics*, vol. 41, no. 5, pp. 1183-1189, 2018, https://doi.org/10.2514/1.G003221.

[39] B. Gao, S. Gao, G. Hu, Y. Zhong, and C. Gu, "Maximum likelihood principle and moving horizon estimation based adaptive unscented Kalman filter," *Science and Technology*, vol. 73, pp. 184-196, 2018, https://doi.org/10.1016/j.ast.2017.12.007.

[40] A. Piwowar and D. Grabowski, "Modelling of the First-Order Time-Varying Filters with Periodically Variable Coefficients," *Mathematical Problems in Engineering*, vol. 2017, 2017, https://doi.org/10.1155/2017/9621651.

[41] R. M. Colorado and L. T. Aguilar, "Robust PID control of quadrotors with power reduction analysis," *ISA Transactions*, vol. 98, pp. 47-62, 2020, https://doi.org/10.1016/j.isatra.2019.08.045.

[42] S. Park, J. Deyst, and J. How, "A new nonlinear guidance logic for trajectory tracking," *AIAA guidance, navigation, and control conference and exhibi*, 2004, https://doi.org/10.2514/6.2004-4900.

[43] W. Hao, B. Xian and T. Xie, "Fault-Tolerant Position Tracking Control Design for a Tilt Tri-Rotor Unmanned Aerial Vehicle," in *IEEE Transactions on Industrial Electronics*, vol. 69, no. 1, pp. 604-612, 2022, https://doi.org/10.1109/TIE.2021.3050384.

[44] A. L. Salih, M. Moghavvemi, H. A. F. Mohamed and K. S. Gaeid, "Modelling and PID controller design for a quadrotor unmanned air vehicle," *2010 IEEE International Conference on Automation, Quality and Testing, Robotics*, pp. 1-5, 2010, https://doi.org/10.1109/AQTR.2010.5520914.

[45] S. K. Singh, A. Sinha and S. R. Kumar, "Nonlinear Control Design for an Unmanned Aerial Vehicle for Path Following," *IFAC-PapersOnLine*, vol. 55, no. 1, pp. 592-597, 2022, https://doi.org/10.1016/j.ifacol.2022.04.097.

[46] A. Eltayeb, M. F. Rahmat, M. A. M. Basri, M. A. M. Eltoum and S. El-Ferik, "An Improved Design of an Adaptive Sliding Mode Controller for Chattering Attenuation and Trajectory Tracking of the Quadcopter UAV," in *IEEE Access,* vol. 8, pp. 205968-205979, 2020, https://doi.org/10.1109/ACCESS.2020.3037557.

[47] H. Bouadi and F. Mora-Camino, "Direct Adaptive Backstepping Flight Control for Quadcopter Trajectory Tracking," *2018 IEEE/AIAA 37th Digital Avionics Systems Conference*, pp. 1-8, 2018, https://doi.org/10.1109/DASC.2018.8569628.

[48] M. S. Mahmoud and M. Maaruf, "Robust Adaptive Multilevel Control of a Quadrotor," in *IEEE Access*, vol. 8, pp. 167684-167692, 2020, https://doi.org/10.1109/ACCESS.2020.3022724.

[49] T. V. Glazkov and A. E. Golubev, "Using Simulink Support Package for Parrot Minidrones in nonlinear control education," *Second international conference on material science, smart structures and application(ICMSS)*, vol. 2195, 2019, https://doi.org/10.1063/1.5140107.

[50] C. S. Subudhi and D. Ezhilarasi, "Modeling and Trajectory Tracking with Cascaded PD Controller for Quadrotor," *Procedia Computer Science*, vol. 133, pp. 952-959, 2018, https://doi.org/10.1016/j.procs.2018.07.082.

[51] E. H. Kadhim and A. T. Abdulsadda, "Improving the Size of the Propellers of the Parrot Mini-Drone and an Impact Study on its Flight Controller System," *International Journal of Robotics and Control Systems*, vol. 3, no. 2 pp. 171-186, 2023, https://doi.org/10.31763/ijrcs.v3i2.933.

[52] A. Baharuddin and M. A. M. Basrii, "Self-Tuning PID Controller for Quadcopter using Fuzzy Logic," *International Journal of Robotics and Control Systems*, vol. 3, no. 3 pp. 728-748, 2023, https://doi.org/10.31763/ijrcs.v3i4.1127.